Ozcan *et al. European Radiology* (2024) 34:6092–6107
https://doi.org/10.1007/s00330-024-10600-2

EUROPEAN SOCIETY OF RADIOLOGY
European Radiology

REVIEW

Current status of optoacoustic breast imaging and future trends in clinical application: is it ready for prime time?

B. Bersu Ozcan[1*], Hashini Wanniarachchi[1], Ralph P. Mason[1] and Basak E. Dogan[1]

Abstract Optoacoustic imaging (OAI) is an emerging field with increasing applications in patients and exploratory clinical trials for breast cancer. Optoacoustic imaging (or photoacoustic imaging) employs non-ionizing, laser light to create thermoelastic expansion in tissues and detect the resulting ultrasonic emission. By combining high optical contrast capabilities with the high spatial resolution and anatomic detail of grayscale ultrasound, OAI offers unique opportunities for visualizing biological function of tissues in vivo. Over the past decade, human breast applications of OAI, including benign/malignant mass differentiation, distinguishing cancer molecular subtype, and predicting metastatic potential, have significantly increased. We discuss the current state of optoacoustic breast imaging, as well as future opportunities and clinical application trends.

Clinical relevance statement Optoacoustic imaging is a novel breast imaging technique that enables the assessment of breast cancer lesions and tumor biology without the risk of ionizing radiation exposure, intravenous contrast, or radionuclide injection.

Key Points

- *Optoacoustic imaging (OAI) is a safe, non-invasive imaging technique with thriving research and high potential clinical impact.*
- *OAI has been considered a complementary tool to current standard breast imaging techniques.*
- *OAI combines parametric maps of molecules that absorb light and scatter acoustic waves (like hemoglobin, melanin, lipids, and water) with anatomical images, facilitating scalable and real-time molecular evaluation of tissues.*

Keywords Photoacoustic techniques, Breast, Cancer

Introduction

The first significant attempt to generate sound from light was described by Alexander Graham Bell in 1880 [1] stimulating various significant events in the development of the technology, as presented in the timeline (Fig. 1). In vivo studies of optoacoustic imaging (OAI) were made possible by advances in methodology and hardware in the 1970s. In OAI, near-infrared, non-ionizing nanosecond laser light pulses induce thermoelastic expansion in tissues generating ultrasonic waves, which are captured by ultrasound transducer/s [2]. Multispectral excitation and unmixing can provide parametric maps of endogenous molecules such as oxyhemoglobin (HbO_2) and deoxyhemoglobin (dHb), melanin, and lipids that absorb light and generate acoustic waves, which can then be fused with anatomic images to allow scalable, relative real-time molecular assessment in tissues [3, 4].

*Correspondence:
B. Bersu Ozcan
BeratBersu.Ozcan@utsouthwestern.edu
[1] Department of Radiology, University of Texas Southwestern Medical Center, 5323 Harry Hines Boulevard MC 8896, Dallas, TX 75390-8896, USA

Springer

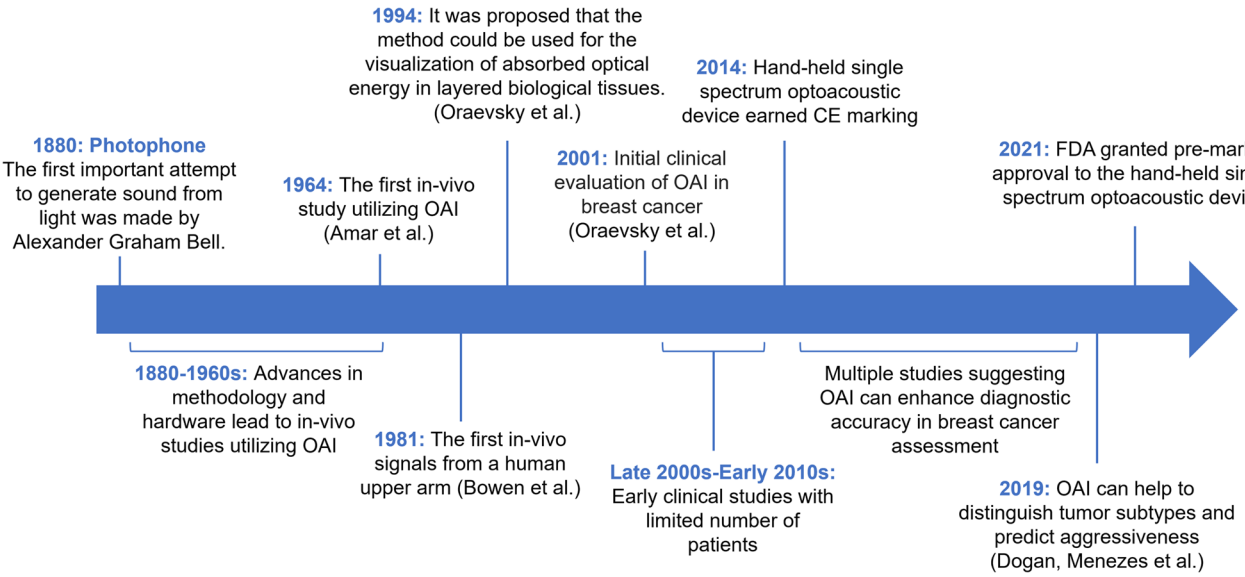

Fig. 1 A history of optoacoustic imaging [1, 3, 4, 7–9, 18, 38, 73–77]. OAI optoacoustic imaging, CE Conformité Européenne

OAI technology leverages both the intrinsic contrast of optical imaging and the acoustic depth of penetration with the high spatial resolution of ultrasound imaging, as recently reviewed [5, 6]. OAI is increasingly used in imaging superficial tissues. In breast imaging, OAI helps distinguish benign and malignant breast lesions, increasing diagnostic specificity in conjunction with grayscale ultrasound [3, 7, 8]. Furthermore, focused imaging of the tumor oxygenation pattern in vivo has been shown to strongly correlate with histopathologic prognostic markers, which shows promise for predictive application of OAI [4]. Herein, we describe the current state of non-contrast-enhanced applications of optoacoustic breast imaging. We review techniques, systems, workflow, and current clinical applications together with limitations and potential future directions.

Principles of optoacoustic imaging (OAI) and commercially available systems

Non-ionizing nanosecond laser pulses are absorbed differentially by different components of the targeted biological tissue and converted to heat. The consequent thermoelastic expansion causes acoustic wave (referred to as optoacoustic waves) emission detected by the wideband US transducers around the tissue. The combination of structural and functional information facilitates the formation of functional and molecular imaging at high resolution, which may be calculated and displayed in real-time.

Different tissue components have unique optical scattering and absorption properties for each wavelength and the use of several wavelengths in OAI helps distinguish them [9]. The main light-absorbing tissue components are oxy- and deoxyhemoglobin (HbO_2 and dHb), lipid, water, and melanin. Since light absorption is concentration-dependent, the detected ultrasound intensity effectively provides a measure of relative concentrations of illuminated molecules [10]. Oxy- and deoxyhemoglobin have distinct absorption spectra, and by selecting appropriate wavelengths for illumination, each can be assessed together with the derived parameters of hemoglobin oxygen saturation (sO_2) and total hemoglobin (HbT). It provides insights into vascular oxygenation and perfusion, as well as hypoxia and angiogenesis which occur during breast cancer development.

Optoacoustic imaging systems can be broadly divided into two types: single-wavelength OAI and multispectral OAI (or multispectral optoacoustic tomography (MSOT)) [11, 12]. Single-wavelength OAI scans can reveal a dominant tissue component such as hemoglobin, though sensitivity and specificity are much improved by using two or more wavelengths [13]. Indeed, MSOT can examine multiple wavelengths, enabling the separation of the complex signals into distinct subcomponents through spectral unmixing [2, 14]. This process facilitates the computation of total blood volume, lipid, and water contributions, alongside measurements of oxy- and deoxyhemoglobin.

Rapidly dividing cancer cells often cause hypoxia and stimulate angiogenesis, making OAI effective at detecting the presence and degree of hypoxia in cancers, relative to normal tissue, and helping distinguish benign from malignant masses [3, 8].

To date, no exogenous contrast agent use in clinical OAI has been reported for breast imaging other than sentinel lymph node detection [15], but several materials approved by the US Food and Drug Administration (FDA) for human use (e.g., indocyanine green, Evans blue, methylene blue) can provide effective photoacoustic contrast.

Optoacoustic breast imaging systems fall into two broad categories: systems with linear arrays or tomographic arrays (Fig. 2). The characteristics of commercial optoacoustic systems for breast imaging are summarized in Table 1. Linear array systems detect photoacoustic waves at limited angles, but are hand-held and portable and have been integrated into existing clinical ultrasound systems. Patients are observed in the supine position. Tomographic systems apply multiple illumination sources around the breast and capture photoacoustic waves emanating from the entire circumference of the breast and generally offer greater depth of signal penetration. The breast is set up in a breast-holding cup when the patient lies on the bed in a prone position. Data are recorded as time-resolved ultrasound signals by multiple ultrasonic transducers distributed around the imaging volume. The association of these transducers with specific spatial locations enables the reconstruction of the imaging volume. 3D systems can provide better sensitivity at greater depth, and can image breast sizes ranging from B cup to DD cup [16].

Advantages of optoacoustic imaging

Optical imaging of the breast suffers from low spatial resolution due to photon scattering, making image interpretation difficult. OAI overcomes this problem by detecting the stimulated US waves, which are combined in a tomographic scheme to generate optical absorption images. Image resolution is determined by the bandwidth of the ultrasound transducer and is limited only by acoustic diffraction. Optoacoustic technology enables laser-based imaging of deeper tissue layers. With low US frequencies (2.25–8 MHz), OAI can produce resolutions of 0.5 to 5 mm at a depth of 3–7 cm [17–19]. Higher US frequency can increase the spatial resolution, but with lower depth penetration due to the increased attenuation of US waves with increasing frequency. This unique scalability contributes to forming images ranging from the microscopic to the macroscopic scale, which is very challenging using other imaging modalities. A strength of OAI is the ability to achieve rudimentary anatomical images and provide co-registered functional and molecular level tissue information without using ionizing radiation or exogenous contrast agents. Furthermore, OAI can be used safely to image patients with metal implants, claustrophobia, or high BMI that limit access to MRI, without the need to use contrast.

Two other modalities that can complement US are ultrasound elastography and microbubble contrast-enhanced ultrasound. Fused ultrasound and optoacoustic imaging with decision support tool assistance showed a lower increase in specificity than has been previously reported for ultrasound elastography, including strain and sheer-wave elastography as shown in recent meta-analysis which ranged from 81 to 88% [20–23]. Of note, there are differences in study design and population, given that studies of elastography included higher numbers of Breast-Imaging Reporting and Data System (BI-RADS) category 2 masses and cysts, whereas OAI studies only included BI-RADS 3, 4, and 5 lesions, where decision-making is more challenging for the radiologist. The previously shown sensitivity range between 80 and 95% as a supplement to US limits its widespread use to down-classify masses [24–26]. Elastography is likely to be used clinically for up-classification or targeted applications, such as differentiating a complicated cyst from a solid mass. Additionally, elastography shows a marked reduction in sensitivity (possibly < 80%) in masses measuring ≤ 1 cm [25, 26]. The observed sensitivity for small vs. larger masses is not significantly different for OAI (masses < 1 cm 96.8%, 98.9% for masses > 2 cm) [23]. This sensitivity for small masses could be particularly important in institutions with supplemental MRI or automated breast ultrasound screening programs, leading to frequent detection of small masses and subsequent need for adjunctive diagnosis and needle biopsies.

(See figure on next page.)

Fig. 2 Schematic illustrations of (**a**) a hand-held linear array optoacoustic system [78], and (**b**) an optoacoustic tomography system equipped with planar [79] and hemispherical [80] arrays. The breast is exposed to non-ionizing, near-infrared laser pulses using either a hand-held dual probe (**a**) or an individual laser source (**b**). The energy is absorbed and converted into heat, resulting in temporary thermoelastic expansion and the emission of ultrasound waves. The generated ultrasonic waves are detected by the hand-held dual probe (**a**), the planar, or hemispherical (**b**) ultrasound (US) transducers, and then analyzed to produce images. A hospital bed was modified to accommodate optoacoustic tomography systems, as depicted in the illustration. In the planar system, the breast is immobilized under mild compression in a craniocaudal direction between a glass window for laser illumination and the US detector array. In the hemispherical system, the breast is held in a hemispherically shaped breast-holding cup filled with body-temperature water. The hemispherical detector under the holding cup detects the ultrasonic emission waves continuously

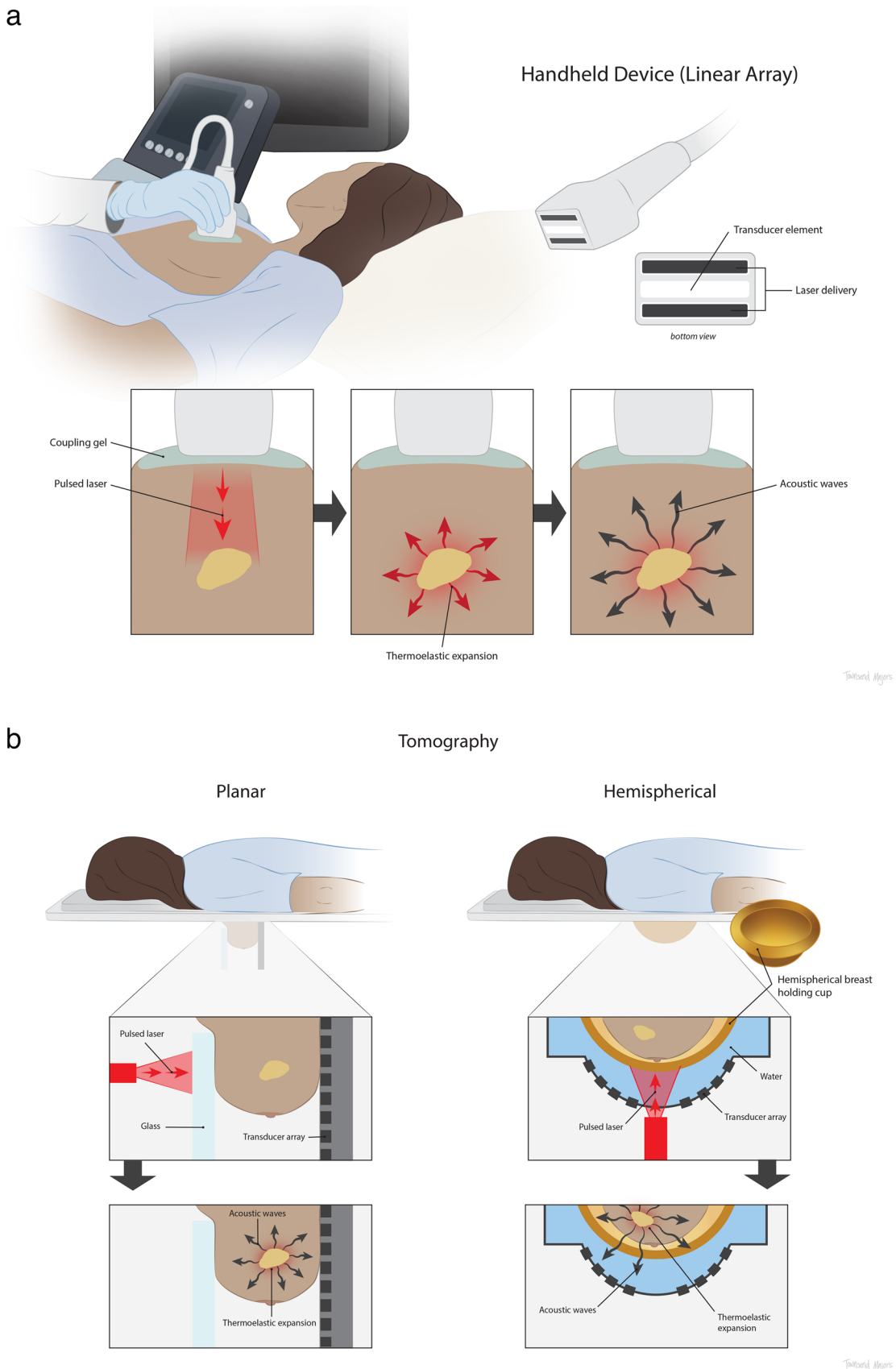

Fig. 2 (See legend on previous page.)

Table 1 Technical characteristics of commercially available clinical optoacoustic breast imaging devices

	MSOT Acuity Echo [43]	Imagio [78]	Single-Breath-Hold Photoacoustic Computed Tomography (SBH-PACT) [16]
Manufacturer	iThera Medical	Seno Medical	CalPACT
FDA approval/CE marking	No FDA approval CE-marked system (since 2019)*	FDA premarket approval CE-marked system (since 2014)	No FDA approval No CE-mark
B-mode ultrasound capability	Yes	Yes	No
Ultrasound detector	*Hand-held 256-element arc-shaped 1D detector array, 2.5–10 MHz	Hand-held 128-element linear 1D detector array, 0.1–12 MHz	Ring 512-element 1D detector array, 2.25 MHz
Penetration depth	Up to 50 mm	Up to 40 mm	Up to 40 mm
Patient position	Supine	Supine	Prone
Laser characteristics	Multispectral optoacoustic tomography (MSOT): 680–980 nm Pulse repetition rate: ≤ 25 Hz	Dual wavelength OAI: 757 and 1064 nm Pulse repetition rate: 5 or 10 Hz	Single-wavelength photoacoustic computed tomography (PACT): 1064 nm Pulse repetition rate: 20 Hz
Resolution	As low as 0.4 mm	Short wavelength, 0.47 mm Long wavelength, 0.42 mm	0.25

MSOT multispectral optoacoustic tomography, *CE* Conformité Européenne, *FDA* Food and Drug Administration

*Hand-held 3D detector available with limited clinical data (not CE-marked)

Similarly, contrast-enhanced US (CEUS) is a potential diagnostic tool for malignant breast tumors due to their generally high vascularization. This method provides real-time information on intralesional vascularization and blood flow by injecting a contrast medium consisting of microbubbles intravenously. CEUS has been shown to improve the diagnostic performance of B-mode US. However, its moderate ability to differentiate benign lesions from malignant ones and the lack of consensus on acquisition and interpretation techniques have prevented its routine use [27, 28]. A meta-analysis by Hu et al revealed that the pooled weighted estimates of sensitivity and specificity for CEUS in the diagnosis of breast lesions were 0.86 and 0.79, respectively, insufficient to obviate needle biopsy in the majority of breast masses [29].

Finally, the current absence of CPT code for OAI hinders predictions concerning the financial impact of this new technology on patients and the overall healthcare system. However, a recent study by Ozcan et al assessed the cost-effectiveness of supplemental use of OAI compared to US alone in distinguishing between benign and malignant breast masses [30]. This evaluation was conducted from the perspective of the US healthcare system in a diagnostic context, and utilized diagnostic test performance parameters from the PIONEER-01 (NCT01943916) clinical trial and cost parameters (USD) from the Truven Health MarketScan Databases [3, 30]. The findings indicated that OAI can cut costs and enhance patient quality of life, mainly by reducing false positives and subsequent benign biopsies [30].

Pitfalls of optoacoustic imaging

As a relatively new technique, OAI is still under development to refine and optimize procedure, protocols, and interpretation. Interpretation of OAI can be challenging due to a lack of technical experience in image acquisition and interpretation, together with needed comprehensive guidelines. This lack of a standardized interpretation system and lexicon makes reporting, and comparing, the results with other breast imaging techniques challenging. Since there is no consensus on the interpretation schema, it remains subjective and operator-dependent. Additionally, converting the optoacoustic (OA) score to a probability of malignancy and BI-RADS category depends on the reader's judgment, adding additional subjectivity to interpretation. Intra- and inter-observer agreement on OAI scores has demonstrated high reliability, and a recent study showed increased accuracy with a machine learning–based decision support tool to address the variability in score interpretation to estimate the probability of malignancy [3, 23].

Progress in source and detector development, such as faster image acquisition at more wavelengths, greater depth penetration, and image reconstruction algorithms, remains an area of active research. There are two major physical artifacts which affect photoacoustic images: fluence and acoustic heterogeneity respectively. Light fluence heterogeneity is caused by superficial layers of an imaging target absorbing photons, lowering the intensity of light which reaches deeper layers. Therefore, the available signal decreases as a function of depth. This nonlinear function, being dependent on the absorption coefficients of different pixels, also varies as a function

of the wavelength and is often referred to as *spectral coloring.*

Acoustic heterogeneity induces problems related to resolution as well as to signal intensity; acoustic waves scatter as they pass through interfaces, and they attenuate according to their frequency. Propagation of acoustic waves may be roughly determined by assuming that the wavefronts propagate along geometrical rays. There are effectively two components to acoustic heterogeneity which affect photoacoustic images: spatially varying speed of sound, and frequency-dependent attenuation.

Another limitation of OAI systems is the current lack of data format uniformity, which impedes data exchange and comparison. This inconsistency hinders overall technological progress in the field and creates obstacles to effective research collaboration among various institutions and researchers. In 2018, the International Photoacoustic Standardization Consortium (IPASC) was formed to standardize test methods and data handling [31]. IPASC's goal is to ensure that data generated by various OAI systems can be easily shared, compared, and analyzed across different platforms, institutions, and research studies in order to improve the reliability and reproducibility of OAI results and foster advancements in the field.

Patient selection considerations

The primary safety concern in OAI is potential damage to tissue due to light exposure [32]. Clinically available devices are within acceptable maximum permissible exposure in accordance with the American National Standards Institute (ANSI) guidelines for the use of lasers in healthcare [3, 7, 33]. Nevertheless, all patients considered for optoacoustic imaging should be routinely screened for a history of any photosensitive disease like porphyria, pellagra, psoriasis, or systemic lupus erythematosus. Patients experiencing photosensitivity associated with a disease or photosensitizing agents such as sulfa, ampicillin, and tetracycline should not be scanned using optoacoustic imaging. The patient should have no open sores, insect bites, or rash on or near the area of the scan.

While melanin is a strong absorber, it did not cause a signal absorption challenge and the use of OAI in Black patients is safe and effective, with outcomes non-inferior to white patients [7]. Furthermore, this technique is deemed safe for patients with breast implants and the presence of implants may enhance the superficiality of breast tissue, potentially leading to improved outcomes.

The impact of lasers on a developing fetus remains unclear [34]. The energy introduced near the fetus during its developmental phase could pose a safety concern, especially since real-time management of the light source and predicting the fetal position can be challenging. FDA premarket approval only applies to non-pregnant women, so non-pregnant status must be confirmed prior to breast OAI [35]. A primary safety concern for OAI is the potential harm to the eyes of patients and scanner staff due to lasers [36]. Class IIIB lasers, which are of intermediate power and emit visible light, can result in retinal damage. Consequently, wearing protective glasses to guard against potential laser exposure is essential.

Evidence for clinical applications in breast imaging

MRI provides important functional information; however, the need to inject contrast to visualize breast cancer and obtain functional data remains a drawback, stimulating search for more effective non-invasive techniques to image breast lesions [37]. OAI provides an alternative to current standard breast imaging techniques and clinical evaluation of optoacoustic breast imaging has accelerated over the past 10 years, including the first studies involving a small number of patients.

Butler et al imaged and scored 94 BI-RADS category 3–5 masses with a linear array optoacoustic imaging system [8]. Each mass was scored by seven blinded independent readers. Internal feature scores were based on total hemoglobin and relative deoxygenation within the tumor. External optoacoustic scores were based on number and orientation of vessels within the boundary zone and number of radiating vessels within the tumor periphery, as well as total hemoglobin and relative deoxygenation within the tumor periphery (Appendix Table 1). This study revealed that both external and internal mean and median optoacoustic scores were higher for malignant masses than for benign masses ($p < 0.0001$) (Figs. 3 and 4) [8].

OAI can improve the specificity of breast mass assessment and decrease benign breast biopsies. In a multisite, prospective study, Menezes et al [38] aimed to compare a linear array optoacoustic imaging system to the device's internal grayscale US alone based on assigned BI-RADS categories. Five blinded independent readers scored five OA features of breast lesions to predict probability of malignancy and then re-assigned a BI-RADS category. Histopathologic diagnosis was considered as the reference standard, and 47.9% (57/119; 95% CI 0.39, 0.57) of BI-RADS 4A and 11.1% (3/27; 95% CI 0.03, 0.28) of BI-RADS 4B were correctly downgraded to BI-RADS 2/3 with OAI while three were incorrectly downgraded for a total of 4.5% false-negative findings. In another multisite, prospective study, seven blinded independent readers assessed 1690 women with 1757 masses [3]. Again, a linear array optoacoustic imaging system was compared to the device's internal grayscale US alone and

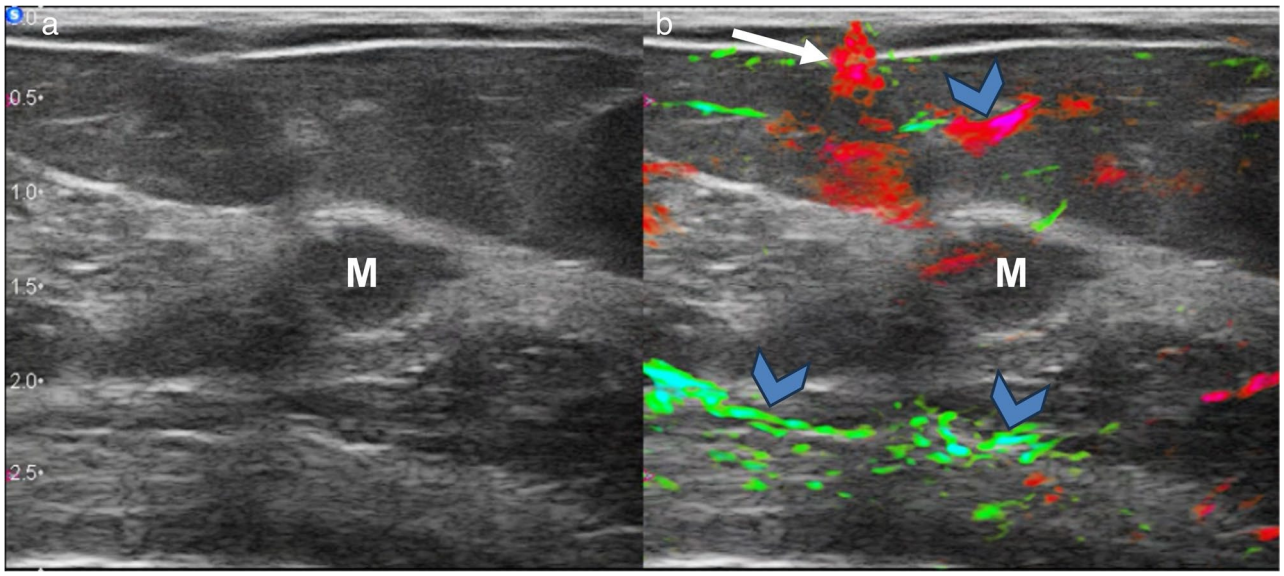

Fig. 3 Images in a 55-year-old woman. **a** Grayscale US image demonstrates an oval hypoechoic mass (M) with lobulated margins assessed as BI-RADS 4B. **b** Fused optoacoustic (OA) and grayscale US image shows absence of internal and external OA features, consistent with benign breast lesion features. Biopsy revealed fibroadenoma. Note the light reflection artifacts parallel to tissue interface (blue arrowheads). Large superficial subcutaneous vessel with OA signal (white arrow). Courtesy: Seno Medical Instruments, Inc. Color map: oxygenation (spectrum of green [most oxygenated] to aqua) and deoxygenation (spectrum of red to pink [most deoxygenated]) of hemoglobin

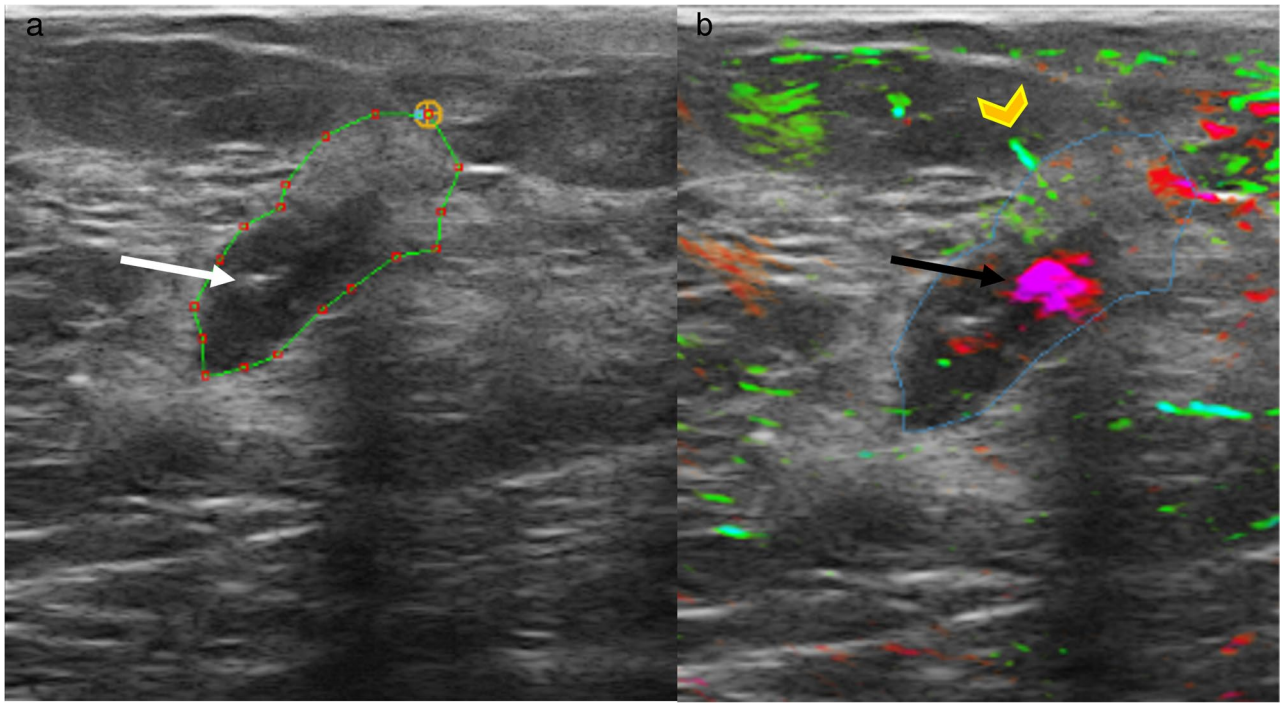

Fig. 4 Images of a breast mass in a 54-year-old woman. **a** Grayscale US demonstrates an oval hypoechoic mass with indistinct margins assessed as BI-RADS 4B. Region of interest in green drawn to indicate tumor margins and central echogenic post biopsy clip is noted (white arrow). **b** Fused grayscale US and OA relative oxygenation parametric map shows large internal tumor vessels within borders demonstrating markedly high levels of deoxyhemoglobin (coded in pink, black arrow), and a few minor border vessels with higher relative oxyhemoglobin (coded in green, orange arrowhead). Biopsy revealed T1N0 invasive cancer (high grade, triple negative). Color map: oxygenation (spectrum of green [most oxygenated] to aqua) and deoxygenation (spectrum of red to pink [most deoxygenated]) of hemoglobin

OAI downgraded 40.8% (3078/7535) benign mass reads and had an absolute specificity advantage of 14.9% over grayscale US ($p < 0.001$) (Fig. 5) [3]. Of note, the number of correct upgrades (1453/4745, 30.6%) was significantly higher than the number of incorrect downgrades (783/4745, 16.5%) among malignant masses ($p < 0.0001$) [3].

OAI can help to distinguish tumor subtypes and predict aggressiveness non-invasively. In a study conducted by Dogan et al, seven readers blinded to molecular characteristics of a total of 532 breast cancers found that total external OA feature scores of luminal (A and B) breast cancers were higher (mean, 9.3 vs. mean, 8.8; $p < 0.05$) and total internal scores were lower (mean, 6.8 vs. mean, 7.7; $p < 0.001$) than those of triple-negative and human epidermal growth factor receptor 2 (HER2)–positive cancers [4]. Also, correlations between higher Ki-67, a breast cancer proliferation marker, and higher internal and lower external optoacoustic feature scores were observed. Better non-invasive differentiation between molecular subtypes is important, since it can affect prognosis and management where triple-negative and HER2-positive cancers benefit more from neoadjuvant chemotherapy [39–41].

OAI can predict the metastatic potential of breast cancers. Breast cancers with metastatic axillary nodes had higher total optoacoustic feature scores compared to cancers without metastasis (mean, 17.3 vs. mean, 12.8; $p < 0.001$) [42]. Furthermore, breast cancers with three or more metastatic nodes had higher optoacoustic feature scores compared to those with no metastasis and low-volume metastasis (mean, 18.5 vs. mean, 10.9; $p < 0.001$).

MSOT has primarily been used in pre-clinical research to date, but its application in translational and clinical research in breast imaging is growing. In a 2017 pilot study, Diot et al [43] used MSOT at 28 wavelengths (700–970 nm) to gain a better understanding of the difference between malignant and nonmalignant breast tissue. They observed that the water and fat lipid layers were disrupted in cancer tissue compared to those in healthy tissue. However, they were less valuable than total blood volume and deoxy-/oxyhemoglobin ratio images showed

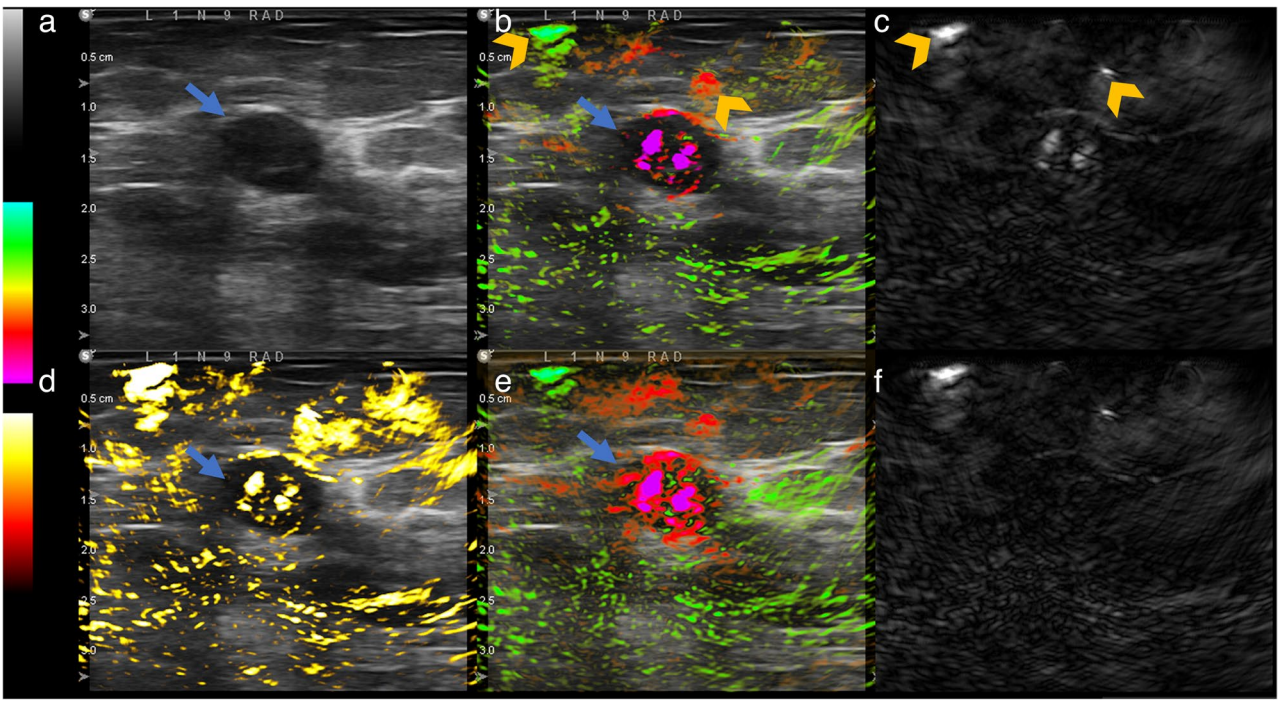

Fig. 5 Images of a mass in a 70-year-old woman. **a** Grayscale US image demonstrates an oval hypoechoic mass with circumscribed margins assessed as BI-RADS-3 (blue arrow). **b** Fused grayscale US and OA image shows internal multiple vessels with hypoxia, and external radiating boundary and peripheral zone vessels with relatively high overall Hb and deoxy Hb content (arrowhead). ACR BI-RADS category was upgraded to BI-RADS 5 by the reader. The large subcutaneous and peritumoral vessels (orange arrowheads) result in light reverberation and reflection artifacts. **c** OA short-wave (757 nm) gray map, which shows relatively more deoxygenated hemoglobin. Vessels utilized in color mapping marked with arrowhead. **d** OA total hemoglobin (yellow) map, with threshold. **e** OA relative map. **f** OA long-wave (1064 nm) gray map, which shows relatively more oxygenated blood. Biopsy revealed invasive ductal carcinoma, triple negative, grade III Ki67 50%. Courtesy: Seno Medical Instruments, Inc. Color map: oxygenation (spectrum of green [most oxygenated] to aqua) and deoxygenation (spectrum of red to pink [most deoxygenated]) of hemoglobin

marked differences between cancer and healthy breast tissue: (1) increased peripheral vascularization and total blood volume heterogeneity compared to normal tissue, (2) high tumor to background total blood volume ratio (up to a 30-fold increase). Table 2 provides a list of recent clinical studies that utilized optoacoustic imaging.

Potential future applications

Assessing tumor hypoxia

Hypoxia, a hallmark of cancer, is associated with tumor aggressiveness and plays a strong role in genetic stability, stimulating angiogenesis and metastasis. It is also pertinent to therapy resistance, notably radiation. While the importance of hypoxia has long been appreciated, there is still no routine clinical procedure for assessing levels of oxygenation in patients' tumors for radiation therapy planning and monitoring the response [44]. Indeed, there remains the mantra "hypoxia: adored and ignored" which may be attributed to the historic lack of suitable methods for assessing tumor hypoxia [45]. Genetic or proteomic signatures of hypoxia have been proposed for the breast and other disease sites based on biopsy specimens [44], but these are necessarily invasive and not practical for assessment of dynamic changes. At the turn of the millennium, polarographic oxygen electrode measurements were promoted, and several studies demonstrated hypoxia in breast tumors [45], which was shown to have some prognostic value for other disease sites such as the cervix [46]. Histography revealed extensive intratumoral heterogeneity and distinct hypoxia compared with normal breast [45]. However, the procedure is highly invasive and time-consuming, required close attention to sampling, and has been largely discontinued. Nuclear medicine approaches based on PET tracers such as [^{18}F]misonidazole (F-MISO) have shown the presence of extensive hypoxia including clinical trials in human breast patients [47]. Quite apart from exposure of patients and staff to radioactivity and the associated costs, PET methods offer relatively low spatial resolution. Examinations may also be time-consuming since optimally they require early and late scans to differentiate perfusion deficit from hypoxia binding effects.

MRI is already included in the radiological workup for some patients and radiomic features have a profound utility for tumor staging [48]. DCE-MRI reveals tumor heterogeneity and relative perfusion and has some prognostic value [48], although routine use of contrast is now discouraged in view of neurofibromatosis syndrome and brain retention. Oxygen-sensitive MRI offers exciting prospects in that the apparent transverse relaxation rate R_2^* is directly influenced by the concentration of deoxyhemoglobin (dHb), as exploited for the foundation of functional MRI (fMRI). Notably, an oxygen gas breathing challenge indicates the ability to enhance tumor oxygenation. In rat breast tumor studies, it was shown that a blood oxygen level dependent (BOLD) signal response was associated with elimination of tumor hypoxia, while tumors showing no signal response remained hypoxic [49]. It was further shown that patients undergoing neoadjuvant chemotherapy (NAC) for locally advanced breast cancer showed superior clinical response if the tumor exhibited a BOLD response to an oxygen gas breathing challenge administered prior to any therapeutic treatment [48]. While BOLD is sensitive to vascular oxygenation, so-called tissue oxygen level dependent (TOLD) or OE-MRI based on spin lattice relaxation rate R_1 is directly sensitive to pO_2. Extensive pre-clinical studies have shown correlations with hypoxia and most recently the ability to stratify rat tumors in terms of radiation response [50]. Significantly such measurements could be performed during radiation treatment planning in an MR-LINAC [51].

OAI is a much newer technology and applications are open to exploration. OAI allows direct assessment of both oxyhemoglobin (HbO_2) and deoxyhemoglobin (dHb), thereby revealing vascular oxygen saturation sO_2 [HbO_2 / (HbO_2 + dHb)] and total hemoglobin (HbO_2 + dHb). This is comparable to BOLD MRI, as rigorously tested by Rich and Seshadri [52], but has the advantage that changes in dHb resulting from vasodilation are readily discriminated from the interconversion of HbO_2 and dHb. Changes in vascular oxygenation monitored by OAI have also been reported with respect to experimental treatments such as vascular-disrupting agents, which caused acute hypoxiation [53, 54], and heme-targeting agents which generated improved vascular oxygenation attributable to vascular paring [55]. Quiros-Gonzalez et al [56] hypothesized that OAI could be used to provide an early indication of response or resistance to antiangiogenic therapy. Testing the MDA-MB-231 in mice, most tumors were found to be resistant to the treatment, but a subset demonstrated a clear survival benefit. At the endpoint, the PAT data from the responding subset showed significantly lower oxygenation and higher hemoglobin content compared with both resistant and control tumors. Moreover, longitudinal analysis revealed that tumor oxygenation diverged significantly in the responding subset, identifying early treatment response and the evolution of different vascular phenotypes between the subsets. The group also found distinct differences in MCF-7 and MDA-MB-231 tumor by OAI, which coincided with histological phenotypes [56].

Examples of rapid acute responses to interventions in MDA-MB-231 breast cancer mouse tumors are presented in Fig. 6, specifically, response to hyperoxic and hypoxic gas breathing challenges. Such measurements

Table 2 A synopsis of recent clinical studies utilizing optoacoustic imaging

Study	Aim	Type	Patients	Outcome
Garcia-Uribe et al (2015) [15]	Sentinel lymph node detection in breast cancer	Single wavelength	Not stated	OAI distinguished sentinel nodes from downstream nodes based on strong optoacoustic contrast from methylene blue.
Diot et al (2017) [43]	Breast mass assessment	MSOT	10 patients with breast cancer, 3 healthy volunteers	Total blood volume (TBV) and deoxy/oxyhemoglobin ratio images showed marked differences between cancer and healthy breast tissue. Tumors had increased peripheral and decreased intratumoral vascularity.
Toi et al (2017) [81]	Breast mass assessment	Dual wavelength	22 patients with breast cancer	OAI detected abnormal peritumoral blood vessels which differ in optoacoustic features.
Lin et al (2018) [16]	Breast mass assessment	Single wavelength	7 patients with breast cancer, 1 healthy volunteer	Single-breath-hold photoacoustic computed tomography identified 8 of the 9 breast cancers by illustrating distinct angiographic anatomy.
Menezes et al (2018) [38]	Breast mass assessment	Dual wavelength	209 patients with 215 breast masses classified as BI-RADS 4A or 4B	47.9% (57/119; 95% CI 0.39, 0.57) of benign masses classified as BI-RADS 4A at US and 11.1% (3/27; 95% CI 0.03, 0.28) of BI-RADS 4B were correctly downgraded to BI-RADS 2/3 with OAI. OAI incorrectly downgraded 4.5% (3/67; 95% CI 0.01, 0.13) of cancers.
Neuschler et al (2018) [7]	Breast mass assessment	Dual wavelength	100 patients with 103 breast masses classified as BI-RADS 3–5	33.7% of false-positive internal grayscale ultrasound reads were downgraded and 87.5% of false-negative internal grayscale ultrasound reads were upgraded. The sensitivity of OAI was 97.1% and the specificity was 44.3%.
Butler et al (2018) [8]	Breast mass assessment	Dual wavelength	92 patients with 94 masses	OAI scores for all individual internal and external features were higher for malignant masses than for benign masses ($p < 0.01$)
Neuschler and Butler et al (2018) [3]	Breast mass assessment	Dual wavelength	1690 patients with 1757 breast masses	OAI exceeded internal grayscale US in specificity by 14.9% ($p < 0.0001$; 99% CI 12.9, 16.9%).
Yamaga et al (2018) [82]	Breast mass assessment	Dual wavelength	22 patients with breast cancer	The vascular branching point counts, up to 7 mm beneath the skin surface, were notably higher in breasts with cancer compared to their unaffected opposite breasts [median, 31.7 (range, 5.87–67.0)/100 cm^2 vs. 27.0 (range, 6.40–44.4)/100 cm^2, respectively, $p < 0.01$].
Dogan and Menezes et al (2019) [4]	Breast cancer molecular subtype assessment	Dual wavelength	519 patients with 532 breast cancers	Total external OAI feature scores of luminal (A and B) breast cancers were higher (9.3 vs. 8.8; $p < 0.05$) and total internal scores were lower (6.8 vs. 7.7; $p < 0.001$) than those of triple-negative and HER2+ cancers.

Table 2 (continued)

Study	Aim	Type	Patients	Outcome
Lin et al (2021) [68]	Neoadjuvant therapy response assessment	Single wavelength	3 patients with 3 breast masses	Single-breath-hold photoacoustic computed tomography demonstrated distinct angiographic structures in the affected breast compared to the healthy one at 3 time points (before, during, and after neoadjuvant therapy).
Nyayapathi et al (2021) [83]	Breast mass assessment	Single wavelength	38 patients with breast cancer	Breasts with tumors had larger-caliber vessels and showed more pronounced variations in background signals compared to the contralateral healthy breasts.
Abeyakoon et al (2022) [84]	Breast mass assessment	Single wavelength	94 patients with 96 breast lesions	OAI had a sensitivity of 96.8% and specificity of 84.6% in detecting breast cancer.
Gu et al (2023) [85]	Sentinel lymph node detection in breast cancer	Single wavelength	11 patients	OAI identified sentinel lymph nodes with a 100% specificity and 52.6% sensitivity.

TBV total blood volume, *OAI* optoacoustic imaging, *US* ultrasound, *MSOT* multispectral optoacoustic tomography, *DOT* diffuse optical tomography, *NAC* neoadjuvant therapy, *pCR* pathologic complete response

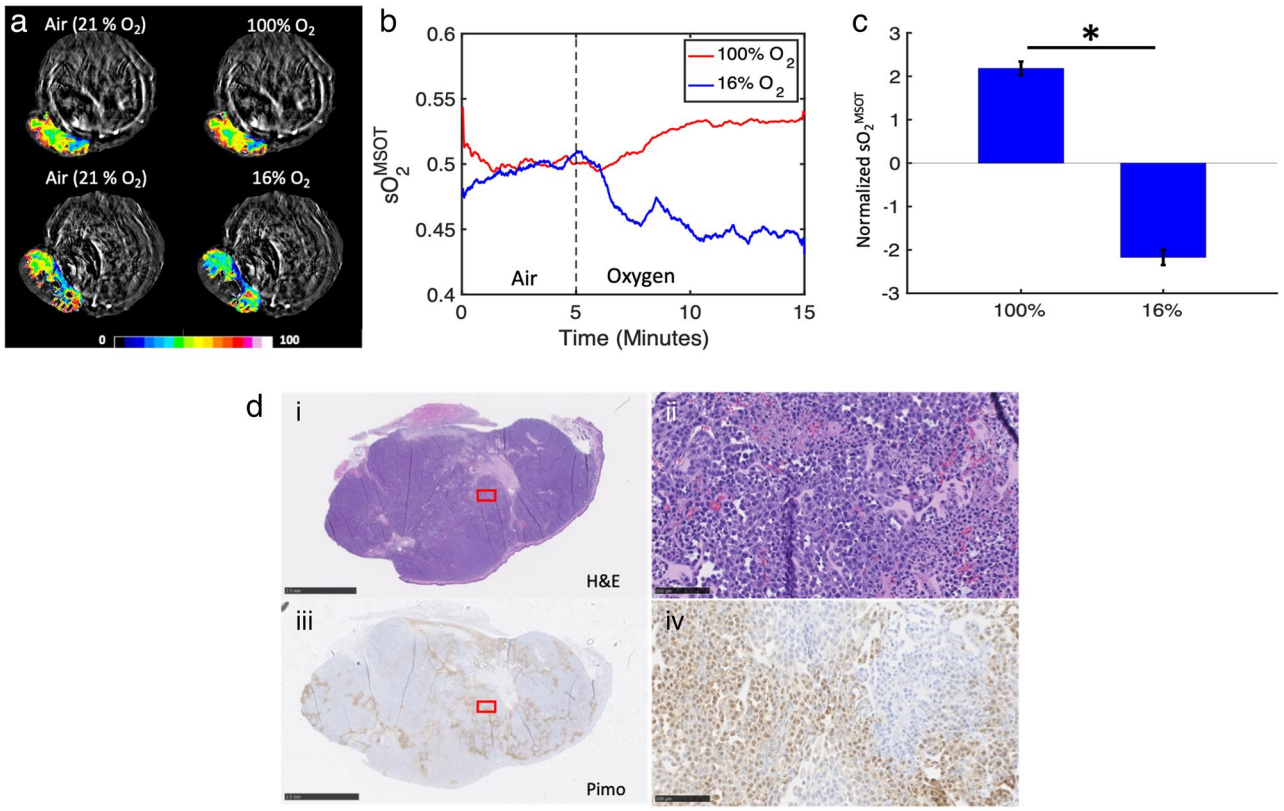

Fig. 6 Detection of changes in vascular oxygenation in response to an intervention in pre-clinical mouse model using MSOT. **a** Transaxial cross-section images of orthotopically implanted MDA-MB-231 breast tumor in upper mammary fat pad with respect to 100% and 16% oxygen gas breathing challenges. Tumor sO_2 distribution is overlaid on anatomical 800 nm MSOT background image. **b** Tumor sO_2 saturation time course. **c** Change in tumor sO_2 during the transition from air to oxygen for 100% and 16% oxygen ($p < 0.05$, *). **d** (i) H&E-stained section of MDA-MB-tumor with (ii) the magnified region, and (iii) pimonidazole-stained section to reveal hypoxic regions of the tumor with (iv) the magnified region. Bars represent 2.5 mm and 100 µm, respectively

are feasible in breast tumor patients and could provide insights into tumor pathophysiology and early indication of treatment response.

Exploring exogenous OAI contrast agents for targeted functional and molecular imaging

Beyond endogenous contrast, specific OAI reporter agents have been demonstrated [6]. The strongest contrast may come from metal nanoparticles, such as gold, which can be targeted to specific receptors such as HER-2. Melanin nanoparticles (MNPs) conjugated with cyclic Arg-Gly-Asp (cRGD) have been used to target integrin $\alpha_v\beta_3$ in pre-clinical breast tumor models (MDA-MB-231) and PyMT to reveal tumor and guide surgical removal of tissue identified via the melanin-induced photoacoustic contrast [57]. In other cases, melanin-doped paclitaxel-loaded albumin nanoparticles have been used to visualize uptake and accumulation in breast tumor xenografts in mice [58]. OAI has also been applied to visualize the location of brachytherapy seeds to verify location of effective radiation distribution in tumors [59]. In terms of radiation, high z-metals such as gold nanoparticles offer a unique opportunity to enhance local radiation dose based on Auger electrons stimulated by tumor irradiation, thereby potentially reducing the required external beam radiation dose, and sparing nearby organs, such as the heart, during breast irradiation, as demonstrated in pre-clinical studies of human tumor xenografts in mice [60, 61]. Such gold nanoparticles are also highly amenable to OAI observation providing a distinct opportunity for imaging providing potential theranostics [62].

Organic chromophores (e.g., 800-CW dye) may also be exploited for tracking agents. Indocyanine green (ICG) can provide strong contrast as a perfusion contrast agent, as explored extensively by Tomaszewski et al [63]. A recent report presented a chromophore, which is directly sensitive to pO_2, whereby the optical lifetime of the so-called nanosphere depends on pO_2 and therefore generates differential ultrasound contrast. Jo et al reported a correlation between photoacoustic lifetime (PALTI) and

radiation damage assessed by γH2AX in a PDX breast tumor model xenograft in mouse [64].

There is also opportunity for instrumentation development. Typically, scans require several seconds for an image acquisition, particularly if specific molecules are to be discriminated (10 to 100 ms per wavelength, and two to five wavelengths). Multiple acquisitions may be acquired to enhance signal to noise ratio; however, motion between individual scans can lead to misregistration corrupting the ability to assess chromophores, such as oxy- or deoxyhemoglobin. Direct acquisition of 3D scans may partially overcome this issue, as well as acquisition of single excitations, allowing co-registration prior to multispectral unmixing [65]. Another potential innovation is incorporation of photoacoustic elastography, which was shown to provide additional ability to identify tumors in some patients [66].

Non-invasive assessment of response to neoadjuvant systemic therapy

Imaging is crucial to evaluating the response to neoadjuvant therapy as a complement to conventional tumor measurements via physical examination. The degree of response can be used as a prognostic tool since pathologic complete response (pCR) is linked to improved disease-free survival [67, 68]. However, no clear clinical practice guidelines exist for assessing tumor response to neoadjuvant therapy. Generally, patients get mammography, US, and a physical exam. In some cases, they also get a DCE-MRI.

An OAI study by Lin et al aimed to evaluate the response to neoadjuvant therapy in three breast cancer patients, with a particular focus on imaging angiographic structures [69]. They utilized single-breath-hold photoacoustic computed tomography to quantify various parameters including cancer size, blood vessel density, entropy, and anisotropy. Notably, distinctive angiographic characteristics were observed in the affected breast when compared to the healthy breast at all three predetermined time points: before, during, and after the treatment. These findings were consistent with the dimension information obtained through conventional imaging techniques as well as the final pathology.

Considering that successful treatment causes cell death well before the tumor cells lyse and are phagocytized by macrophages, it is likely that functional changes within and around the tumor may precede size changes assessed by conventional imaging. Studies with diffuse optical spectroscopy, which uses near-infrared light to provide spectral information about tissue microstructure and functional parameters including oxygenated and deoxygenated hemoglobin, have demonstrated that changes in oxygenation occur as early as 24 h following the beginning of treatment in responders [70–72]. A clinical trial (ClinicalTrials.gov Identifier: NCT05337280) is currently underway to investigate the feasibility of OAI to detect pathologic complete response. Dogan and her team aim to evaluate whether OAI can detect changes in the amount of hemoglobin and relative oxygenation/deoxygenation of hemoglobin before changes in size are seen on grayscale (B-mode) ultrasound and whether these achieve better sensitivity and/or specificity in predicting pathologic complete response.

Conclusion

OAI is a new imaging technique using non-ionizing laser illumination to fuse functional and anatomic imaging in conjunction with US with promising applications to the human breast. Parametric maps allow scalable, relative real-time molecular assessment of tissue hypoxia and can be used to gain information about breast cancer aggressiveness and tumor biology without the risk of ionizing radiation exposure, intravenous contrast, or radionuclide injection. The main limitations of OAI are the depth limit (~3–7 cm), scatter artifacts, and the lack of an objective interpretation schema. Furthermore, the relatively higher cost of devices compared to US alone and lack of familiarity of the radiologist with OAI imaging features may limit its use in the clinic.

OAI is a safe, non-invasive imaging technique with thriving research and high demonstrated clinical impact. Larger multicenter cohort studies and clinical trials are needed to establish the observed trends and accelerate its clinical translation.

Abbreviations

BI-RADS	Breast-Imaging Reporting and Data System
BOLD	Blood oxygen level dependent
dHb	Deoxyhemoglobin
HbO_2	Oxyhemoglobin
HER2	Human epidermal growth factor receptor 2
MRI	Magnetic resonance imaging
MSOT	Multispectral optoacoustic tomography
NIR	Near-infrared
OAI	Optoacoustic imaging
PET	Positron emission tomography
TOLD	Tissue oxygen level dependent
US	Ultrasound

Supplementary Information

The online version contains supplementary material available at https://doi.org/10.1007/s00330-024-10600-2.

Below is the link to the electronic supplementary material. Supplementary file1 (PDF 63 KB)

Acknowledgements

We would like to thank Townsend Majors for her help in illustrating the optoacoustic device systems.

Funding
Dr. Ozcan is fully supported by Eugene P. Frenkel Scholarship in Clinical Medicine granted to Dr. Dogan by UT Southwestern Simmons Comprehensive Cancer Center. The study presented in Fig. 6 was supported in part by NIH NCI grants 1R01CA244579, 2P30CA142543, and S10 OD018094.

Declarations

Guarantor
The scientific guarantor of this publication is Basak E. Dogan, MD.

Conflict of interest
The authors of this manuscript declare relationships with the following companies: Basak E. Dogan, MD, received a research grant from Seno Medical Instruments for an unrelated project regarding neoadjuvant chemotherapy response assessment. Seno Medical Instruments, Inc. is the source of the cases described in Figs. 3 and 5.

Statistics and biometry
No complex statistical methods were necessary for this paper.

Informed consent
Written informed consent was not required for this study because this is a review study.

Ethical approval
Institutional Review Board approval was not required because this is a review study.

Study subjects or cohorts overlap
No study subjects or cohorts have been previously reported.

Methodology

- review
- performed at one institution

Received: 8 September 2023 Revised: 7 December 2023
Accepted: 26 December 2023 Published online: 3 February 2024

References

1. Alexander GB. On the production and reproduction of sound by light: [read before the American Association for the Advancement of Science, in Boston, August 27, 1880.] (1880) Researches of Sumner Tainter and Alexander Graham Bell. Photophonic transmitters. Experiments to ascertain the nature of the rays that affect selenium. Non-Electric Photophonic Receivers. Ame J Sci 20(118):305
2. Ntziachristos V, Ripoll J, Wang LV, Weissleder R (2005) Looking and listening to light: the evolution of whole-body photonic imaging. Nat Biotechnol 23(3):313–20
3. Neuschler EI, Butler R, Young CA et al (2018) A pivotal study of optoacoustic imaging to diagnose benign and malignant breast masses: a new evaluation tool for radiologists. Radiology 287(2):398–412
4. Dogan BE, Menezes GLG, Butler RS et al (2019) Optoacoustic imaging and gray-scale US features of breast cancers: correlation with molecular subtypes. Radiology 292(3):564–572
5. Zhang J, Duan F, Liu Y, Nie L (2020) High-resolution photoacoustic tomography for early-stage cancer detection and its clinical translation. Radiol Imaging Cancer 2(3)
6. MacCuaig WM, Jones MA, Abeyakoon O, McNally LR (2020) Development of multispectral optoacoustic tomography as a clinically translatable modality for cancer imaging. Radiol Imaging Cancer. 2(6)
7. Neuschler EI, Lavin PT, Tucker FL et al (2018) Downgrading and upgrading gray-scale ultrasound BI-RADS categories of benign and malignant masses with optoacoustics: a pilot study. AJR Am J Roentgenol 211(3):689–700
8. Butler R, Lavin PT, Tucker FL et al (2018) Optoacoustic breast imaging: imaging-pathology correlation of optoacoustic features in benign and malignant breast masses. AJR Am J Roentgenol 211(5):1155–1170
9. Zackrisson S, van de Ven SMWY, Gambhir SS (2014) Light in and sound out: emerging translational strategies for photoacoustic imaging. Cancer Res. 74(4):979–1004
10. Dolet A, Ammanouil R, Petrilli V et al (2021) In vitro and in vivo multispectral photoacoustic imaging for the evaluation of chromophore concentration. Sensors (Basel). 21(10):3366
11. Wen Y, Guo D, Zhang J et al (2022) Clinical photoacoustic/ultrasound dual-modal imaging: current status and future trends. Front Physiol 13:1036621
12. Nyayapathi N, Xia J (2019) Photoacoustic imaging of breast cancer: a mini review of system design and image features. J Biomed Opt 24(12):1–13
13. Tzoumas S, Nunes A, Deliolanis NC, Ntziachristos V (2015) Effects of multispectral excitation on the sensitivity of molecular optoacoustic imaging. J Biophotonics 8(8):629–637
14. Buehler A, Kacprowicz M, Taruttis A, Ntziachristos V (2013) Real-time handheld multispectral optoacoustic imaging. Opt Lett 38(9):1404–6
15. Garcia-Uribe A, Erpelding TN, Krumholz A et al (2015) Dual-modality photoacoustic and ultrasound imaging system for noninvasive sentinel lymph node detection in patients with breast cancer. Sci Rep 5:15748
16. Lin L, Hu P, Shi J et al (2018) Single-breath-hold photoacoustic computed tomography of the breast. Nat Commun 9(1):2352
17. Kim C, Erpelding TN, Jankovic L, Pashley MD, Wang LV (2010) Deeply penetrating in vivo photoacoustic imaging using a clinical ultrasound array system. Biomed Opt Express 1(1):278–284
18. Manohar S, Dantuma M (2019) Current and future trends in photoacoustic breast imaging. Photoacoustics 16:100134
19. Kruger RA, Lam RB, Reinecke DR, Del Rio SP, Doyle RP (2010) Photoacoustic angiography of the breast. Med Phys 37(11):6096–6100
20. Barr RG, De Silvestri A, Scotti V et al (2019) Diagnostic performance and accuracy of the 3 interpreting methods of breast strain elastography: a systematic review and meta-analysis. J Ultrasound Med 38(6):1397–1404
21. Pillai A, Voruganti T, Barr R, Langdon J (2022) Diagnostic accuracy of shear-wave elastography for breast lesion characterization in women: a systematic review and meta-analysis. J Am Coll Radiol 19(5):625-634.e0
22. Barr RG, Engel A, Kim S, Tran P, De Silvestri A (2023) Improved breast 2D SWE algorithm to eliminate false-negative cases. Invest Radiol 58(10):703–709
23. Seiler SJ, Neuschler EI, Butler RS, Lavin PT, Dogan BE (2023) Optoacoustic imaging with decision support for differentiation of benign and malignant breast masses: a 15-reader retrospective study. AJR Am J Roentgenol 220(5):646–658
24. Pu H, Zhang XL, Xiang LH et al (2019) The efficacy of added shear wave elastography (SWE) in breast screening for women with inconsistent mammography and conventional ultrasounds (US). Clin Hemorheol Microcirc 71(1):83–94
25. Sadigh G, Carlos RC, Neal CH, Wojcinski S, Dwamena BA (2013) Impact of breast mass size on accuracy of ultrasound elastography vs conventional B-mode ultrasound: a meta-analysis of individual participants. Eur Radiol 23(4):1006–1014
26. Suvannarerg V, Chitchumnong P, Apiwat W et al (2019) Diagnostic performance of qualitative and quantitative shear wave elastography in differentiating malignant from benign breast masses, and association with the histological prognostic factors. Quant Imaging Med Surg 9(3):386–398
27. Du J, Wang L, Wan CF et al (2012) Differentiating benign from malignant solid breast lesions: combined utility of conventional ultrasound and contrast-enhanced ultrasound in comparison with magnetic resonance imaging. Eur J Radiol 81(12):3890–3899
28. Liu H, Jiang YX, Liu JB, Zhu QL, Sun Q (2008) Evaluation of breast lesions with contrast-enhanced ultrasound using the microvascular imaging technique: initial observations. Breast 17(5):532–539
29. Hu Q, Wang XY, Zhu SY, Kang LK, Xiao YJ, Zheng HY (2015) Meta-analysis of contrast-enhanced ultrasound for the differentiation of benign and malignant breast lesions. Acta Radiol 56(1):25–33
30. Ozcan BB, Xi Y, Dogan BE (2023) Supplemental optoacoustic imaging of breast masses: a cost-effectiveness analysis. Acad Radiol 31(1):121–130

31. Gröhl J, Hacker L, Cox BETAL (2022) The IPASC data format: a consensus data format for photoacoustic imaging. Photoacoustics 26:100339
32. Xu M, Wang LV (2006) Photoacoustic imaging in biomedicine. Review of scientific instruments 77(4):041101
33. Menke J (2015) Photoacoustic breast tomography prototypes with reported human applications. Eur Radiol 25(8):2205–2213
34. Wilkerson EC, Van Acker MM, Bloom BS, Goldberg DJ (2019) Utilization of laser therapy during pregnancy: a systematic review of the maternal and fetal effects reported from 1960 to 2017. Dermatol Surg 45(6):818–828
35. Premarket Approval (PMA). U.S. Food and Drug Administration website. Available via https://www.accessdata.fda.gov/scripts/cdrh/cfdocs/cfpma/pma.cfm?id=P200003. Updated May 15, 2023. Accessed May 18, 2023.
36. Laser Safety Information. The Laser Institute website. Available via https://www.lia.org/resources/laser-safety-information. Accessed October 4, 2023
37. Mann RM, Hooley R, Barr RG, Moy L (2020) Novel approaches to screening for breast cancer. Radiology 297(2):266–285
38. Menezes GLG, Pijnappel RM, Meeuwis C et al (2018) Downgrading of breast masses suspicious for cancer by using optoacoustic breast imaging. Radiology 288(2):355–365
39. Kim YJ, Kim JS, Kim IA (2018) Molecular subtype predicts incidence and prognosis of brain metastasis from breast cancer in SEER database. J Cancer Res Clin Oncol 144(9):1803–1816
40. Early Breast Cancer Trialists' Collaborative Group (EBCTCG) (2005) Effects of chemotherapy and hormonal therapy for early breast cancer on recurrence and 15-year survival: an overview of the randomised trials. Lancet 365(9472):1687–717
41. Yin L, Duan JJ, Bian XW, Yu SC (2020) Triple-negative breast cancer molecular subtyping and treatment progress. Breast Cancer Res 22(1):61
42. Presented by Dogan et al at the 108th Scientific Assembly and Annual Meeting of the Radiological Society of North America, November 29 to December 5, 2020.
43. Diot G, Metz S, Noske A et al (2017) Multispectral optoacoustic tomography (MSOT) of human breast cancer. Clin Cancer Res 23(22):6912–6922
44. Buffa FM, Harris AL, West CM, Miller CJ (2010) Large meta-analysis of multiple cancers reveals a common, compact and highly prognostic hypoxia metagene. Br J Cancer 102(2):428–435
45. Vaupel P, Schlenger K, Knoop C, Höckel M (1991) Oxygenation of human tumors: evaluation of tissue oxygen distribution in breast cancers by computerized O2 tension measurements. Cancer Res 51(12):3316–3322
46. Fyles A, Milosevic M, Hedley D et al (2002) Tumor hypoxia has independent predictor impact only in patients with node-negative cervix cancer. J Clin Oncol 20(3):680–687
47. Daimiel I (2019) Insights into hypoxia: non-invasive assessment through imaging modalities and its application in breast cancer. J Breast Cancer 22(2):155–171
48. Panico C, Ferrara F, Woitek R et al (2022) Staging breast cancer with MRI, the T. A key role in the neoadjuvant setting. Cancers (Basel) 14(23)
49. Zhao D, Jiang L, Hahn EW, Mason RP (2009) Comparison of 1H blood oxygen level-dependent (BOLD) and 19F MRI to investigate tumor oxygenation. Magn Reson Med 62(2):357–364
50. Arai TJ, Yang DM, Campbell JW et al (2021) Oxygen-sensitive MRI: a predictive imaging biomarker for tumor radiation response? Int J Radiat Oncol Biol Phys 110(5):1519–1529
51. Dubec MJ, Buckley DL, Berks M et al (2023) First-in-human technique translation of oxygen-enhanced MRI to an MR Linac system in patients with head and neck cancer. Radiother Oncol 183:109592
52. Rich LJ, Seshadri M (2015) Photoacoustic imaging of vascular hemodynamics: validation with blood oxygenation level-dependent MR imaging. Radiology 275(1):110–118
53. Liu L, O'Kelly D, Schuetze R (2021) Non-invasive evaluation of acute effects of tubulin binding agents: a review of imaging vascular disruption in tumors. Molecules 26(9)
54. Guo Y, Wang H, Gerberich JL et al (2021) Imaging-guided evaluation of the novel small-molecule benzosuberene tubulin-binding agent KGP265 as a potential therapeutic agent for cancer treatment. Cancers (Basel) 13(19)
55. Ghosh P, Guo Y, Ashrafi A et al (2020) Oxygen-enhanced optoacoustic tomography reveals the effectiveness of targeting heme and oxidative phosphorylation at normalizing tumor vascular oxygenation. Cancer Res 80(17):3542–3555
56. Quiros-Gonzalez I, Tomaszewski MR et al (2022) Photoacoustic tomography detects response and resistance to bevacizumab in breast cancer mouse models. Cancer Res 82(8):1658–1668
57. Liu JJ, Wang Z, Nie LM (2022) RGD-functionalised melanin nanoparticles for intraoperative photoacoustic imaging-guided breast cancer surgery. Eur J Nucl Med Mol Imaging 49(3):847–860
58. Sim C, Kim H, Moon H, Lee H, Chang JH, Kim H (2015) Photoacoustic-based nanomedicine for cancer diagnosis and therapy. J Control Release 203:118–125
59. Harrison T, Zemp RJ (2011) Coregistered photoacoustic-ultrasound imaging applied to brachytherapy. J Biomed Opt 16(8):080502
60. Wu Z, Stangl S, Hernandez-Schnelzer A et al (2023) Functionalized hybrid iron oxide-gold nanoparticles targeting membrane Hsp70 radiosensitize triple-negative breast cancer cells by ROS-mediated apoptosis. Cancers (Basel) 15(4)
61. Nosrati H, Salehiabar M, Charmi J et al (2023) Enhanced in vivo radiotherapy of breast cancer using gadolinium oxide and gold hybrid nanoparticles. ACS Appl Bio Mater 6(2):784–792
62. Schuemann J, Berbeco R, Chithrani DB et al (2016) Roadmap to clinical use of gold nanoparticles for radiation sensitization. Int J Radiat Oncol Biol Phys 94(1):189–205
63. Tomaszewski MR, Gehrung M, Joseph J, Quiros-Gonzalez I, Disselhorst JA, Bohndiek SE (2018) Oxygen-enhanced and dynamic contrast-enhanced optoacoustic tomography provide surrogate biomarkers of tumor vascular function, hypoxia, and necrosis. Cancer Res 78(20):5980–5991
64. Jo J, Folz J, Gonzalez ME et al (2023) Personalized oncology by in vivo chemical imaging: photoacoustic mapping of tumor oxygen predicts radiotherapy efficacy. ACS Nano 17(5):4396–4403
65. O'Kelly D, Guo Y, Mason RP (2020) Evaluating online filtering algorithms to enhance dynamic multispectral optoacoustic tomography. Photoacoustics 19:100184
66. Biswas D, Vasudevan S, Chen GCK, Bhagat P, Sharma N, Phatak S (2017) Time–frequency based photoacoustic spectral response technique for differentiating human breast masses. Biomed Phys Eng Express 3(3):035002
67. von Minckwitz G, Untch M, Blohmer JU (2012) Definition and impact of pathologic complete response on prognosis after neoadjuvant chemotherapy in various intrinsic breast cancer subtypes. J Clin Oncol 30(15):1796–1804
68. Cortazar P, Zhang L, Untch M et al (2014) Pathological complete response and long-term clinical benefit in breast cancer: the CTNeoBC pooled analysis. Lancet 384(9938):164–172
69. Lin L, Tong X, Hu P, Invernizzi M, Lai L, Wang LV (2021) Photoacoustic computed tomography of breast cancer in response to neoadjuvant chemotherapy. Adv Sci (Weinh) 8(7):2003396
70. Schaafsma BE, van de Giessen M, Charehbili A et al (2015) Optical mammography using diffuse optical spectroscopy for monitoring tumor response to neoadjuvant chemotherapy in women with locally advanced breast cancer. Clin Cancer Res 21(3):577–584
71. Roblyer D, Ueda S, Cerussi A et al (2011) Optical imaging of breast cancer oxyhemoglobin flare correlates with neoadjuvant chemotherapy response one day after starting treatment. Proc Natl Acad Sci U S A 108(35):14626–14631
72. Ntziachristos V, Chance B (2001) Probing physiology and molecular function using optical imaging: applications to breast cancer. Breast Cancer Res 3(1):41–46
73. Amar L, Bruma M, Desvignes P, Leblanc M, Perdriel G, Velghe M (1964) Detection d'omes elastiques (ultrasonores) sur l'os occipital, induites par impulsions laser dans l'oeil d'un lapin. C R Hebd Seances Acad Sci 259:3653–3655
74. Bowen T, Nasoni RL, Pifer AE, Sembroski GH. (1981) Some experimental results on the thermoacoustic imaging of tissue equivalent phantom materials. in Proceedings 1981 Ultrasonics Symposium. IEEE 823–827.
75. Oraevsky AA, Jacques SL, Esenaliev RO, Tittel FK (1994) Laser-based optoacoustic imaging in biological tissues. in Laser-tissue interaction V and ultraviolet radiation hazards. SPIE 2134:122–128
76. Oraevsky AA, Karabutov AA, Solomatin SV et al (2001) Laser optoacoustic imaging of breast cancer in vivo. In Biomed Pptoacoustics II SPIE 4256:6–15
77. Menezes GLG, Mann RM, Meeuwis C et al (2019) Optoacoustic imaging of the breast: correlation with histopathology and histopathologic biomarkers. Eur Radiol 29(12):6728–6740

78. Oraevsky AA, Clingman B, Zalev J, Stavros AT, Yang WT, Parikh JR (2018) Clinical optoacoustic imaging combined with ultrasound for coregistered functional and anatomical mapping of breast tumors. Photoacoustics 12:30–45
79. Manohar S, Kharine A, van Hespen JC, Steenbergen W, van Leeuwen TG (2005) The Twente Photoacoustic Mammoscope: system overview and performance. Phys Med Biol 50(11):2543–2557
80. Kruger RA, Kuzmiak CM, Lam RB, Reinecke DR, Del Rio SP, Steed D (2013) Dedicated 3D photoacoustic breast imaging. Med Phys 40(11):113301
81. Toi M, Asao Y, Matsumoto Y et al (2017) Visualization of tumor-related blood vessels in human breast by photoacoustic imaging system with a hemispherical detector array. Scientific Rep 7(1):41970
82. Yamaga I, Kawaguchi-Sakita N, Asao Y et al (2018) Vascular branching point counts using photoacoustic imaging in the superficial layer of the breast: a potential biomarker for breast cancer. Photoacoustics 11:6–13
83. Nyayapathi N, Zhang H, Zheng E et al (2021) Photoacoustic dual-scan mammoscope: results from 38 patients. Biomed Opt Express 12(4):2054–2063
84. Abeyakoon O, Woitek R, Wallis MG et al (2022) An optoacoustic imaging feature set to characterise blood vessels surrounding benign and malignant breast lesions. Photoacoustics 27:100383
85. Gu L, Deng H, Bai Y et al (2023) Sentinel lymph node mapping in patients with breast cancer using a photoacoustic/ultrasound dual-modality imaging system with carbon nanoparticles as the contrast agent: a pilot study. Biomed Opt Express 14(3):1003–1014

Publisher's Note